Applied and Computational Mechanics 6 (2012) 5–16

Determination of Lamb wave dispersion curves by means of Fourier transform

P. Hora[a,*], O. Červená[a]

[a] *Institute of Thermomechanics of the ASCR, v.v.i., Veleslavínova 11, 301 14 Plzeň, Czech Republic*

Received 13 June 2011; received in revised form 29 March 2012

Abstract

This work reports on methods for determination of Lamb wave dispersion curves by means of Fourier transform (FT). Propagating Lamb waves are sinusoidal in both the frequency domain and the spatial domain. Therefore, the temporal FT may be carried out to go from the time to the frequency domain, and then the spatial FT may be carried out to go to the *frequency–wave-number* domain, where the amplitudes and the wave-numbers of individual modes may be measured. The result of this transform will be a 2D array of amplitudes at discrete frequencies and wave-numbers. Other method of determination of dispersion curves is based on the solution of FEM task in frequency domain. The frequency spectrum of a time-dependent excitation is defined using FT. Since a small number of frequencies are sufficient to achieve a correct representation of a wide variety of temporal excitations, this approach considerably speeds up the computation by avoiding the temporal FT and by decreasing the number of calculation steps.

Keywords: Lamb wave, dispersion curves, Fourier transform, FEM

1. Introduction

The application of the conventional ultrasonic methods, such as pulse-echo, has been limited to testing relatively simple geometries or interrogating the region in the immediate vicinity of the transducer. A new ultrasonic methodology uses guided waves to examine structural components [10]. The advantages of this technique include: its ability to test the entire structure in a single measurement; and its capability to test inaccessible regions of complex components.

The propagation of guided waves in a complex structure is a complicated process that is difficult to understand and interpret. The current research develops the mechanics fundamentals that model this propagation.

One approach to the modeling of guided wave propagatiǹ phenomena is to solve the governing differential equations of motion and their associated boundary conditions analytically. This procedure has been already done for simple geometries and perfect specimens without defects (see [7] and [11]). However, these equations become intractable for more complicated geometries or for non-perfect specimens.

A numerical solution is another approach to this problem. A number of different numerical computational techniques can be used for the analysis of wave propagation. These include finite difference equations, finite element methods (FEM), finite strip elements [4], boundary element methods, global matrix approaches [9], spectral element methods [8], mass-spring lattice models [13] and the local interaction simulation approach [6]. The primary advantage of

*Corresponding author. Tel.: +420 377 236 415, e-mail: hora@cdm.it.cas.cz.

the FEM is that there are numerous available commercial FEM codes, which eliminates any need to develop actual code.

Comparison between dispersion curves of a perfect structure and dispersion curves of a defect structure is main feature of the guided wave method. This work reports on methods for determination of Lamb wave dispersion curves by means of Fourier transform.

2. Theory

Lamb waves are two-dimensional vibrations propagating in plates with free boundary conditions. Their displacements may be symmetric or antisymmetric with respect to the middle plane of the plate. Sometimes they are referred to as free or normal modes, because they are the eigensolutions of characteristic equations. The velocities of all Lamb waves are dispersive. The frequency equation for the propagation of symmetric waves is

$$\frac{\tan \beta h}{\tan \alpha h} = -\frac{4\alpha\beta k^2}{(k^2-\beta^2)^2} \tag{1}$$

and the frequency equation for the propagation of antisymmetric waves is

$$\frac{\tan \beta h}{\tan \alpha h} = -\frac{(k^2-\beta^2)^2}{4\alpha\beta k^2}, \tag{2}$$

where $\alpha^2 = \omega^2/c_1^2 - k^2$, $\beta^2 = \omega^2/c_2^2 - k^2$, k is wavenumber, ω is angular frequency, c_1, c_2 are phase velocities (subscripts refer to wave mode: 1-longitudinal, 2-shear) and h is half-thickness of the plate [7]. Dispersion curves for symmetric (1) and antisymmetric (2) modes for phase velocities are shown in Fig. 1 – left and for group velocities you can see in Fig. 1 – right.

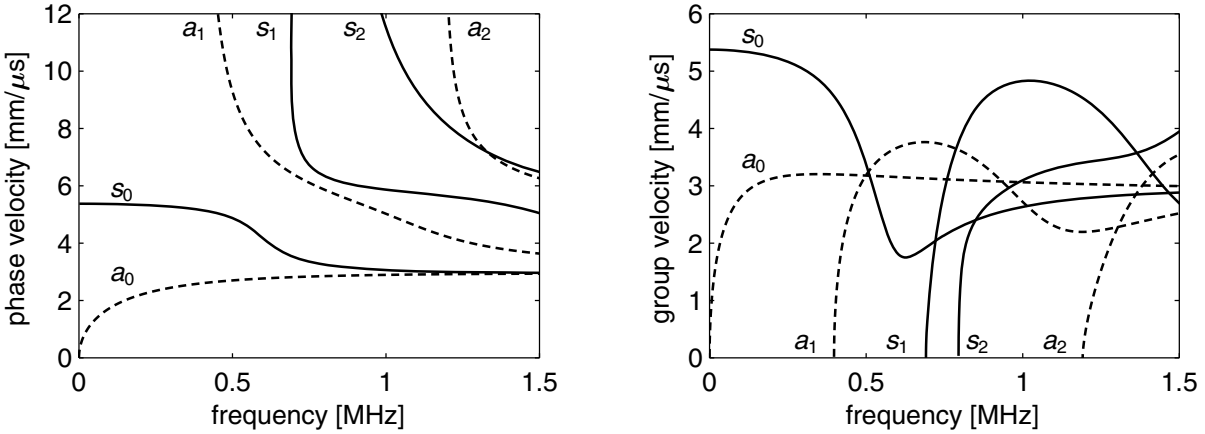

Fig. 1. Velocity dispersion curves for steel, where $c_1 = 5\,950$ m/s and $c_2 = 3\,180$ m/s; symmetric modes $s_0 \ldots s_2$ (solid lines), antisymmetric modes $a_0 \ldots a_2$ (dashed lines)

The displacements corresponding to the symmetric modes are given by

$$\begin{aligned} u_x &= A\, i\beta \left(\frac{\cos \beta y}{\cos \beta h} - \frac{2k^2 \cos \alpha y}{(k^2-\beta^2)\cos \alpha h} \right) \mathrm{e}^{i(kx-\omega t)}, \\ u_y &= A\, k \left(\frac{\sin \beta y}{\cos \beta h} + \frac{2\alpha\beta \sin \alpha y}{(k^2-\beta^2)\cos \alpha h} \right) \mathrm{e}^{i(kx-\omega t)} \end{aligned} \tag{3}$$

and the displacements corresponding to the antisymmetric modes are

$$\begin{aligned} u_x &= A\, i\beta \left(\frac{\sin \beta y}{\sin \beta h} - \frac{2k^2 \sin \alpha y}{(k^2 - \beta^2) \sin \alpha h} \right) \mathrm{e}^{i(kx - \omega t)}, \\ u_y &= A\, k \left(\frac{\cos \beta y}{\sin \beta h} + \frac{2\alpha\beta \cos \alpha y}{(k^2 - \beta^2) \sin \alpha h} \right) \mathrm{e}^{i(kx - \omega t)}, \end{aligned} \tag{4}$$

where x, y are spatial coordinates, t is time, i is imaginary unit and A is constant [7].

Since the propagating Lamb waves are sinusoidal in both the frequency domain and the spatial domain, the temporal FT may be carried out to go from the time to the frequency domain, and then the spatial FT may be carried out to go to the *frequency–wave-number* domain, where the amplitudes and the wave-numbers of individual modes may be measured.

Applying the spatial Fourier methods in practice to data gained experimentally or numerically requires us to carry out a two-dimensional FT giving

$$H(k, f) = \int_{-\infty}^{+\infty} \int_{-\infty}^{+\infty} u(x, t) \mathrm{e}^{-i(kx + \omega t)} \, \mathrm{d}x \, \mathrm{d}t. \tag{5}$$

The discrete 2D FT may be defined similarly to the 1D FT. The result of this transform will be a 2D array of amplitudes at discrete frequencies and wave-numbers. As in the one-dimensional case, aliasing must be avoided by sampling the data at a sufficiently high frequency both in time and in wave number space. Usually, the signal will be not periodic within the temporal and spatial sampling windows and leakage will occur. Window functions such as the Hanning window may be used to reduce this leakage, and zeros may be padded to the end of the signal to enable the frequency and wave number of the maximum amplitude to be determined more accurately.

The algorithm of time analysis is following [1]:

1. Create the array (in column order) from experimentally or numerically gained the time histories of the waves received at a series of equally spaced positions along the propagation path.
2. Carry out the temporal FT of each column to obtain a frequency spectrum for each position. At this stage, an array with the spectral information for each position in its respective column is obtained.
3. Carry out the spatial FT of each row formed by the components at a given frequency to obtain the *frequency–wave-number* information.

In the case of frequency analysis the frequency spectra in particular places on the surface of the plate are available. Therefore it is sufficient to carry out only the spatial FT

$$H(k, f) = \int_{-\infty}^{+\infty} u(x, f) \mathrm{e}^{-ikx} \, \mathrm{d}x \tag{6}$$

for obtaining *frequency–wave-number* information.

Then the algorithm is following:

1. Create the array (in column order) from gained the complex displacement for each frequency received at a series of equally spaced positions along the propagation path.
2. Carry out the spatial FT of each row to obtain the *frequency–wave-number* diagram.

3. Numerical simulations

FEM calculations are performed in the commercial environment COMSOL Multiphysics with the Structural Mechanics Module [5]. The plane strain is used as an application mode. The analyzed steel plate is $2h = 4\,\text{mm}$ thick and $L = 120\,\text{mm}$ long. Young's modulus $E = 205\,\text{GPa}$, Poisson's ratio $\nu = 0.30$ and density $\rho = 7\,800\,\text{kg/m}^3$. The plate geometry and the used coordinate system are shown in Fig. 2. The mapped squared mesh with size of elements $0.5 \times 0.5\,\text{mm}$ is created. Elements are of the Lagrange–Quadratic type. The exciting constraint is set at the left edge of this plate. The others edges are free.

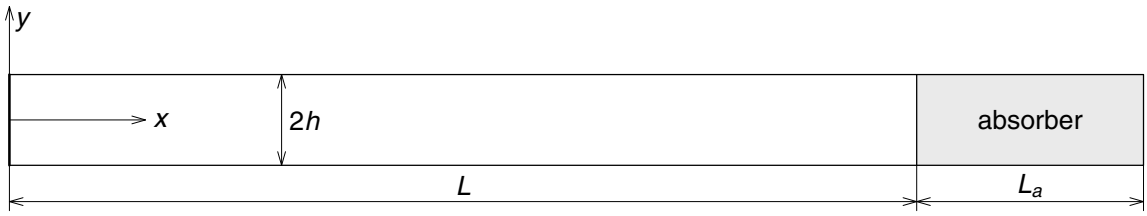

Fig. 2. The plate geometry and the used coordinate system

Two kinds of problems are realized: firstly, the time dependent analysis, and secondly, the frequency response analysis. The time stepping parameters for time dependent analysis are: times (from 0 to 100 with step $0.01\,\mu$s), relative tolerance (10^{-5}) and absolute tolerance (10^{-10}). For frequency analysis, $L_a = 20\,\text{mm}$ long absorbing part is appended to the main plate [3]. The Young's modulus of this absorbing part is complex, given by function $E_A = E\,(1 + i\,1\,500(x - L)^2)$, where i is imaginary unit and x is the position in x direction.

Exciting pulse

An individual Lamb wave is temporary launched from one end of the plate sinusoidal tone burst, modulated temporary by a Hanning window function to limit bandwidth. This time pulse is given by relation

$$f(t) = \frac{1}{2}\,(1 - \cos(\omega_0 t/N_c))\,\sin(\omega_0 t), \qquad t \in \langle 0, N_c/f_0\rangle, \tag{7}$$

where f_0 is center frequency, ω_0 is center angular frequency, N_c is the number of cycles and t is time. The spectrum of pulse envelope is

$$\int_0^{N_c/f_0} (1 - \cos(\omega_0 t/N_c))\;\mathrm{e}^{-i\omega t}\,\mathrm{d}t = \frac{4i\pi^2 f_0^2\left(\mathrm{e}^{i\,\omega\frac{N_c}{f_0}} - 1\right)\mathrm{e}^{-i\omega\frac{N_c}{f_0}}}{\omega\,(\omega^2 N_c^2 - 4\pi^2 f_0^2)}. \tag{8}$$

The numerical tests are done for the number of cycles 3, 5 and 7 and for the center frequencies from 0.1 MHz to 1 MHz with step 0.1 MHz. Presented results are for $N_c = 5$ and $f_0 = 0.5\,\text{MHz}$. Fig. 3 shows the time history of such pulse and the amplitude spectrum of its envelope.

The amplitude of u_x and u_y displacement of exciting pulse at each node at the plate edge are given by the through thickness deflected shape calculated from (3) or (4) for center frequency. The examples of the u_x and u_y displacements for the first antisymmetric mode (a_0) and the first symmetric mode (s_0) and frequencies 0.31, 0.5 and 0.69 MHz are shown in Fig. 4.

Note that in this way of exciting the modes are pure only at the center frequency of the imposed excitation signal. This is to be expected as the imposed displacement deflected shapes

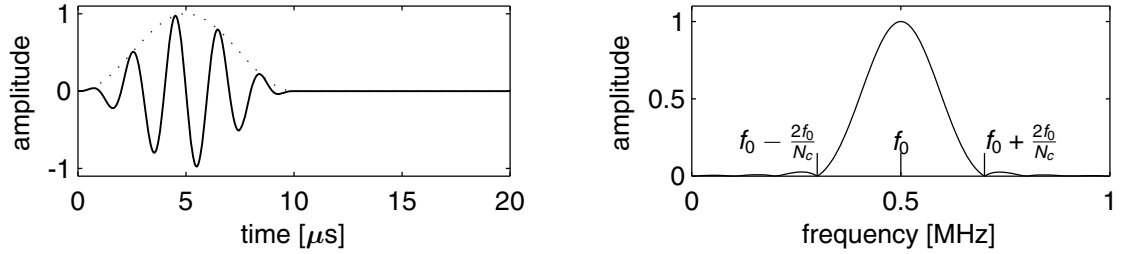

Fig. 3. Time history of pulse used in numerical tests (left) and amplitude spectrum of its envelope (right)

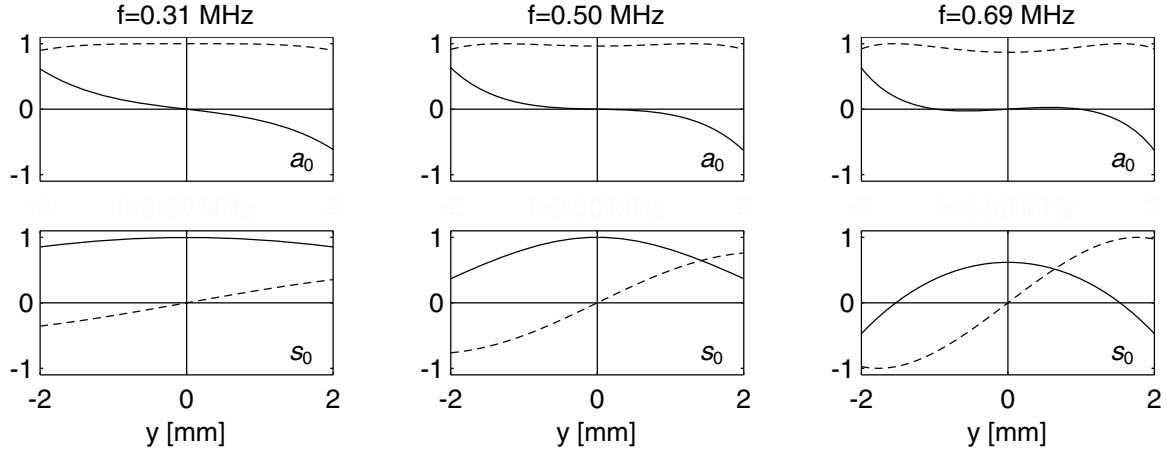

Fig. 4. The deflected mode shapes of Lamb waves a_0 and s_0 for the lowest, central and the highest frequency; u_x displacement (solid line), u_y displacement (dashed line)

shown in Fig. 4 – center were correct only at 0.5 MHz and as may be deduced from (3) and (4) the mode shapes are slightly different either side of this frequency. Hence, the frequency dependence of the mode shapes means that excitation signals of the form shown in Fig. 3 – left will generally excite more than one mode away from their center frequencies. Pure a_0 and s_0 modes may be excited at a frequency below the frequency of the first non-zero propagating modes a_1 and s_1 respectively if the input signal is symmetric in the x direction and antisymmetric in the y direction for s_0 and vice versa for a_0.

In order to excite a pure Lamb wave two conditions have to be simultaneously satisfied [2]. Firstly, the frequency of the harmonic excitation signal must be identical to the Lamb wave frequency being excited and secondly, the variation of the excitation with y at the excitation position ($x = 0$ in the test reported here) must correspond to the exact mode shape of the Lamb wave being excited. Assuming a single frequency input, the required excitation $\boldsymbol{f}(y,t)$ is of the form

$$\boldsymbol{f}(y,t) = \boldsymbol{\Phi}(y)\,\mathrm{e}^{i\omega t} \tag{9}$$

and $\boldsymbol{\Phi}(y) = [u_x, u_y]^\top$ may be calculated from (3) and (4).

However, in almost all modeling applications single frequency excitation is not desirable or possible, for example in explicit time marching FE methods the duration of the input signal has to be finite. It is therefore very advantageous to be able to excite single modes with a wideband excitation signal $f(t)$. This can be achieved by summing the required inputs over a range of frequencies. For single frequency component ω_j, the required input is

$$\boldsymbol{f}_j(y,t) = \boldsymbol{\Phi}_j(y) A(\omega_j)\,\mathrm{e}^{i\omega_j t}. \tag{10}$$

If all the significant energy components in the excitation signal are over a range of frequencies from $j = 1$ to k then

$$\boldsymbol{f}(y,t) = \sum_{j=1}^{k} \boldsymbol{\Phi}_j(y) A(\omega_j)\, \mathrm{e}^{i\omega_j t}. \tag{11}$$

Here, $A(\omega)$ is the complex amplitude of the Fourier transform of the excitation signal $f(t)$, where $f(t)$ is a tone burst modified by Hanning window in the tests reported here. This method of exciting Lamb waves in the numerical investigation is hence adopted in all the temporal FE simulations that follow.

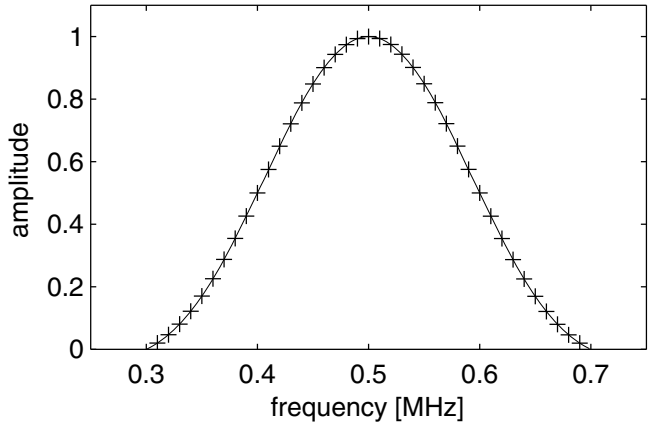

Fig. 5. Frequency spectrum

The frequency spectrum of this temporal waveform is quite narrow, see Fig. 5. The crosses in this figure indicate 39 discrete frequency components used for the FE analysis in frequency domain. The u_x and u_y displacement of excitation at each node at the left edge of the plate were given by the through thickness deflected shape calculated from (3) or (4) for given frequency. Then the displacements were multiplied by the corresponding amplitude of frequency spectrum.

Tests of the velocity predictions

A set of simple tests was carried out to velocity predictions obtained using COMSOL Multiphysics. The tests were proceeded on an extremely simple system. This was $2h = 0.5$ mm thick and $L = 300$ mm long steel plate, see Fig. 2. The phase velocities for steel were: $c_1 = 5\,950$ m/s and $c_2 = 3\,180$ m/s.

All surface nodes were pinned in the y direction. The plate was therefore effectively infinite in the y and z directions, so simple plane wave propagation could be expected. A 0.5 mm square mesh was used. The plate was excited by applying the signal shown in Fig. 3 – left in the x direction to all the nodes at $x = 0$. This excited the bulk longitudinal wave. Fig. 6 – left shows the response of the top surface of the plate in the x direction at distance $x = 100$ mm. The shape of the waveform is the same as the input shown in the Fig. 3 – left indicating that the numerical scheme has not introduced dispersion. Using the time flight between the two monitored points the velocity was calculated as $5\,917.2$ m/s. The model was then modified. The surface nodes were pinned in the x direction now. This allowed a pure shear wave to propagate along the plate. A y direction displacement of the form shown in Fig. 3 – left was applied to each of the nodes at $x = 0$ and the resulting predicted waveform at $x = 100$ mm is shown in Fig. 6 – right. Again, no dispersion is evident and using the time flight between the two monitored points the

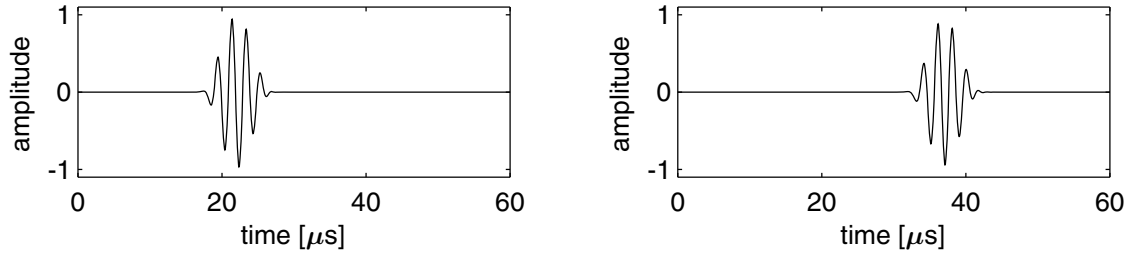

Fig. 6. Predicted time history at time $x = 100$ mm, when the input at $x = 0$ was excited: the longitudinal wave c_1 only (left), the shear wave c_2 only (right)

velocity was calculated as $3\,159.6$ m/s. In all the above cases, the FE predictions are excellent and the velocities differed from the theoretically predicted ones by less than 1 % confirming the applicability of the finite element program COMSOL Multiphysics.

Results from temporal analysis

As mentioned above, a wideband excitation signal $\boldsymbol{f}(y,t)$ given by (11) was applied for center frequency $f_0 = 0.5$ MHz. Amplitude of vertical displacements in dependence on space and time is illustrated by pseudocolor plot in Fig. 7. The case when the left edge of the plate was loaded by displacements equivalent to the first antisymmetric mode (a_0) (see Fig. 4 – central above) is shown at the left side and the case when the left edge of the plate was loaded by displacements equivalent to the first symmetric mode (s_0) (see Fig. 4 – central bottom) is shown on the right side. These results are obtained by FEM calculations. The Fig. 8 shows the pseudocolor plot of *frequency–wave-number* spectrum, which was computed by 2D FT in MATLAB [12]. The dispersion curves obtained analytically are plotted by solid lines (symmetric mode) and dashed lines (antisymmetric mode). Negative values of wave-number correspond to the waves propagating from left to right edge of the plate and positive values to the waves propagating in opposite direction. Note that two antisymmetric modes (a_0, a_1) exist at given frequency (0.5 MHz).

Results from frequency analysis

Other method of dispersion curves determination is based on the solution of FEM task in frequency domain. The frequency spectrum of a time-dependent excitation was defined using FT. Then, the structure response (complex displacements and stresses at any locations) was calculated at each frequency of this load, i.e. the FE-code supplies stationary solution for each frequency component of the temporal excitation. The Fig. 9 shows the pseudocolor plot of *frequency–wave-number* spectrum, which was computed by 1D FT in MATLAB. The solid lines refer to symmetric modes and the dashed lines refer to antisymmetric modes of the analytically obtained dispersion curves. Negative values of wave-number correspond to the waves propagating from left to right edge of the plate again. The reflected waves practically do not exist because of presence of the absorber. Almost no spectral values exist in the area of positive wave-number values.

4. Experiment

The 2D FT algorithm was verified by the experimentally gained data. The experiment was performed at the Ultrasonic methods department of the Institute of Thermomechanics AS CR. The measurement of vertical displacements on surface of the steel plate was the object of the experiment.

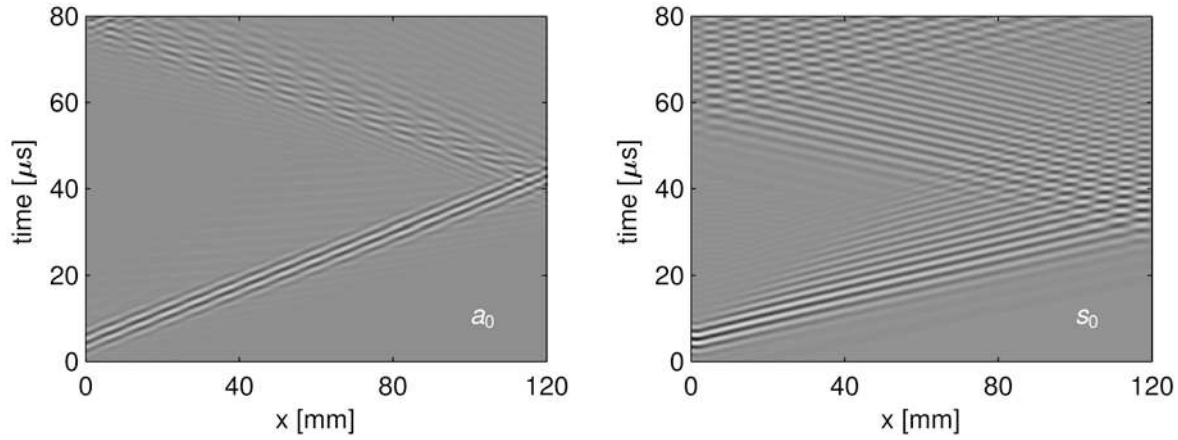

Fig. 7. *Time-spatial* distribution of vertical displacement when input at $x = 0$ was designed a_0 (left) or s_0 (right) only

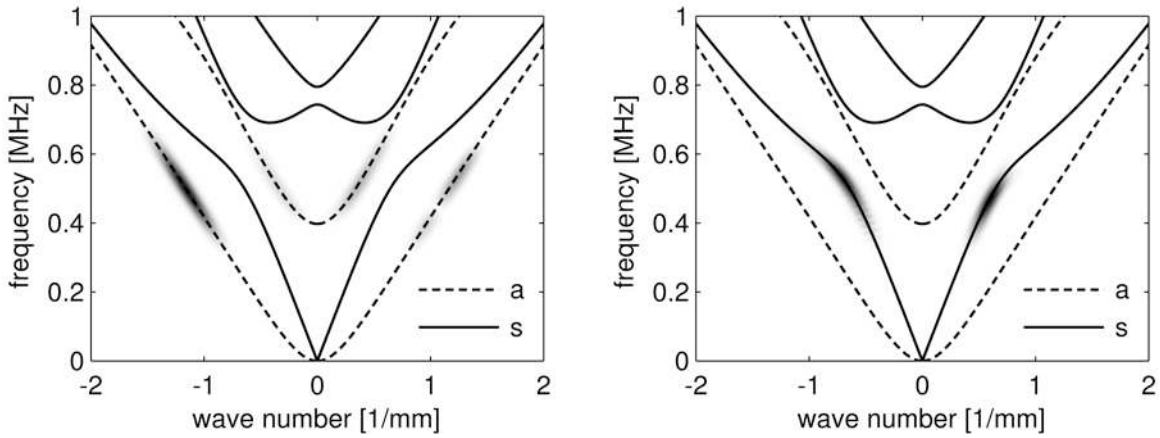

Fig. 8. *Frequency–wave-number* distribution after 2D FT when input at $x = 0$ was designed a_0 (left) or s_0 (right) only

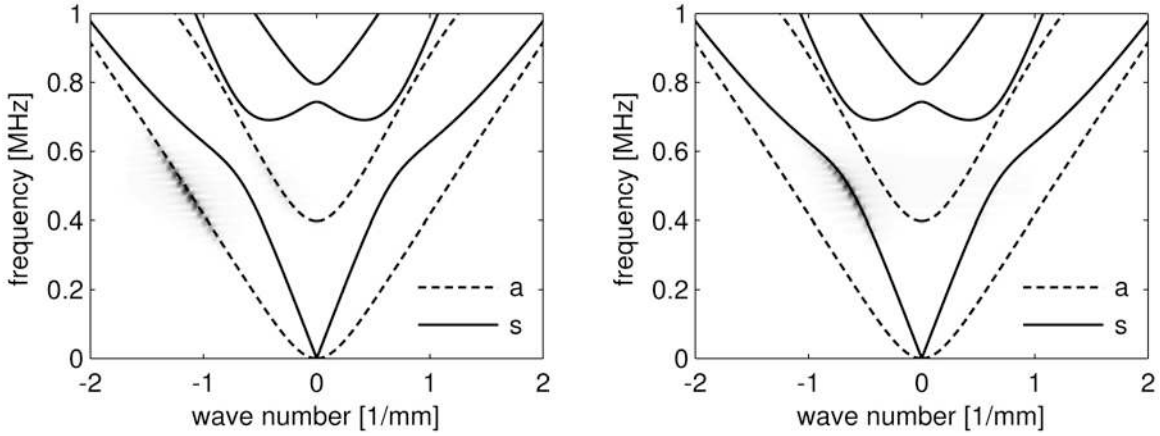

Fig. 9. *Frequency–wave-number* distribution after 1D FT when input at $x = 0$ was designed a_0 (left) or s_0 (right) only

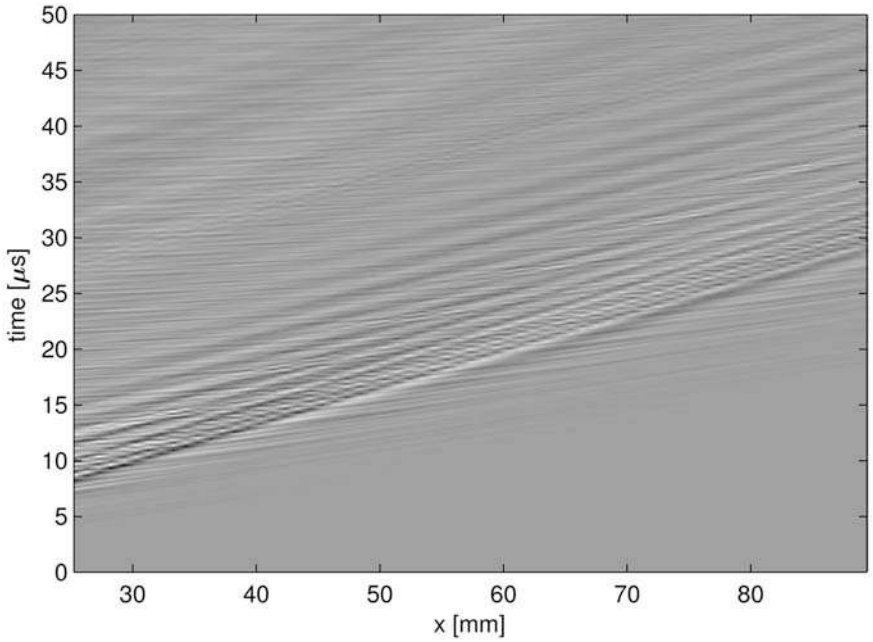

Fig. 10. *Time-spatial* distribution of vertical displacement on surface of the steel plate for the laser excitation

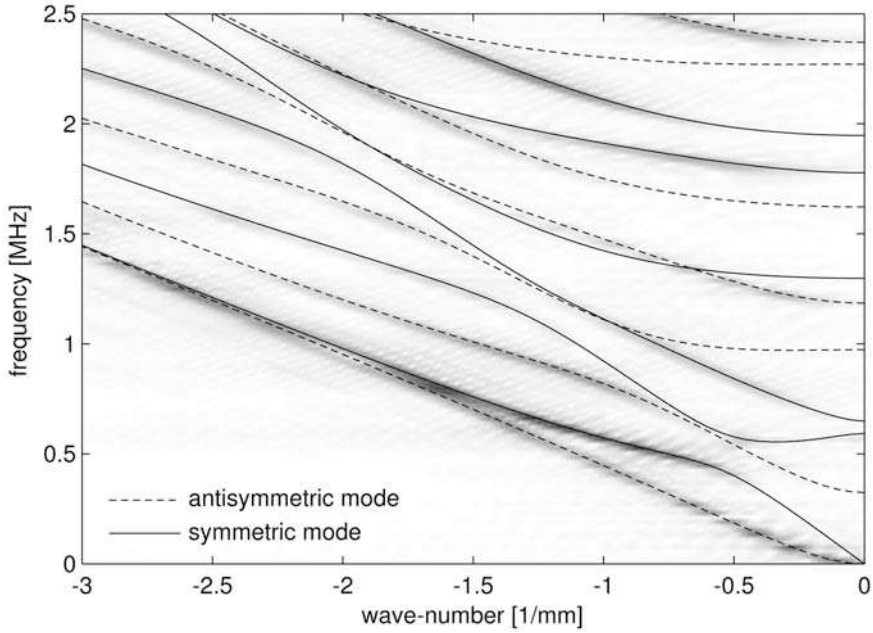

Fig. 11. *Frequency–wave-number* distribution after 2D FT of experimental data on surface of the steel plate

The steel plate size was $280.2 \times 280.4 \times 5.04$ mm. The measured mechanical properties of the plate were $c_1 = 5\,973.3$ m/s, $c_2 = 3\,270.6$ m/s, Poisson's ratio $\nu = 0.285\,9$ and density $\rho = 7\,793$ kg/m^3. The laser source of excitation was placed in the center of the plate. The displacements were scanned on the plate surface in distance 25.25 to 89.4 mm (with step $1.002\,3$ mm) from the center of the plate by the miniature transducers (the VP-1093 Pinducer). The digital oscilloscope LeCroy 9304AM was used for recording of the transducer signals.

The vertical displacements in dependence on space and time are illustrated by pseudocolor plot in Fig. 10. The Fig. 11 shows the pseudocolor plot of *frequency–wave-number* spectrum,

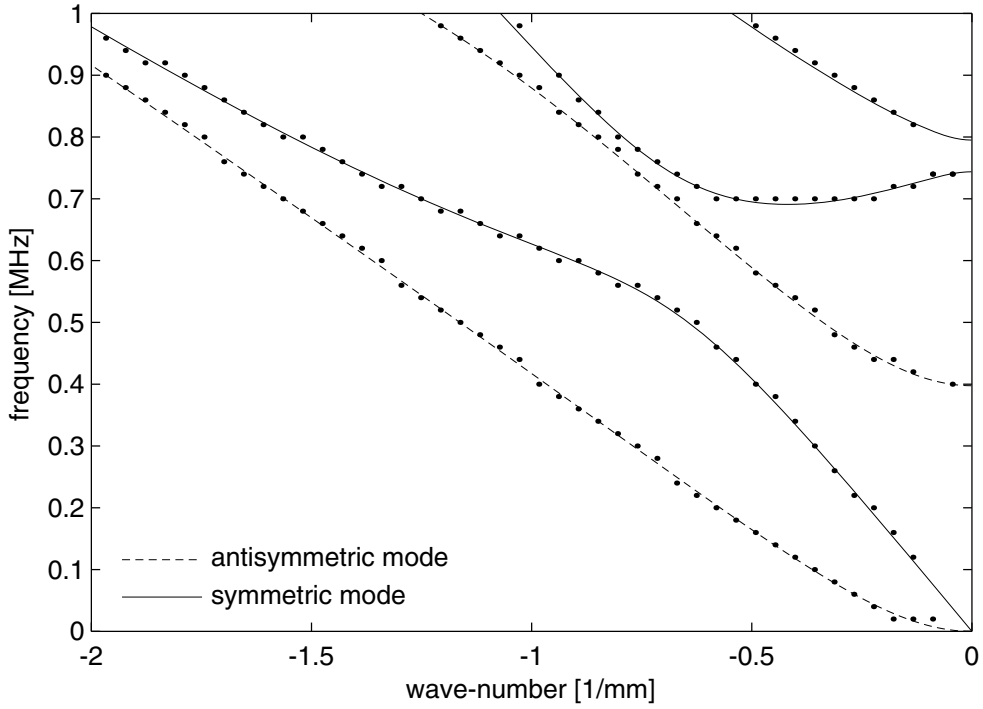

Fig. 12. Estimation of dispersion curves by the frequency method

which was computed by 2D FT in MATLAB. The dispersion curves obtained analytically for given testing plate are plotted by solid lines (symmetric mode) and dashed lines (antisymmetric mode). Negative values of wave-number correspond to the waves propagating from center of the plate. The experimental data do not contain reflected waves than positive values of wave-number are not considered. Note that there are many both symmetric and antisymmetric excited modes in wide range of frequencies. It is caused by very narrow laser pulse. The most significant are the first symmetric and antisymmetric modes.

5. Determination of dispersion curves

In this section dispersion curves in a thick plate were determined by means of FEM task in frequency domain and following 1D FT. The geometry of the plate, its elastic constants and mesh parameters were the same as in section 3. The plate was excited at the left edge by constant constrain. Because of more accurate determination of particular modes, the task was divided into two parts: identification of symmetric modes and identification of antisymmetric ones. The symmetric modes were excited by displacement in x direction; the antisymmetric modes were excited by displacement in y direction. The value of displacement was $1\,\mu$m for both cases. FEM task was performed for frequencies from 20 kHz to 1 MHz with step 20 kHz.

The dots in Fig. 12 represent the peak values of *frequency–wave-number* spectrum, which was computed by the spatial FT of the frequency spectra in particular places on the surface of the plate. The dispersion curves obtained analytically are plotted for verification by solid lines (symmetric mode) and dashed lines (antisymmetric mode).

Note that the dispersion curves obtained by means of FEM are in good agreement with the dispersion curves computed analytically. The accuracy of the dispersion curves determination is sufficient for an ultrasonic methodology using guided waves to examine structural components. The accuracy is possible to increase by decreasing of the frequency step.

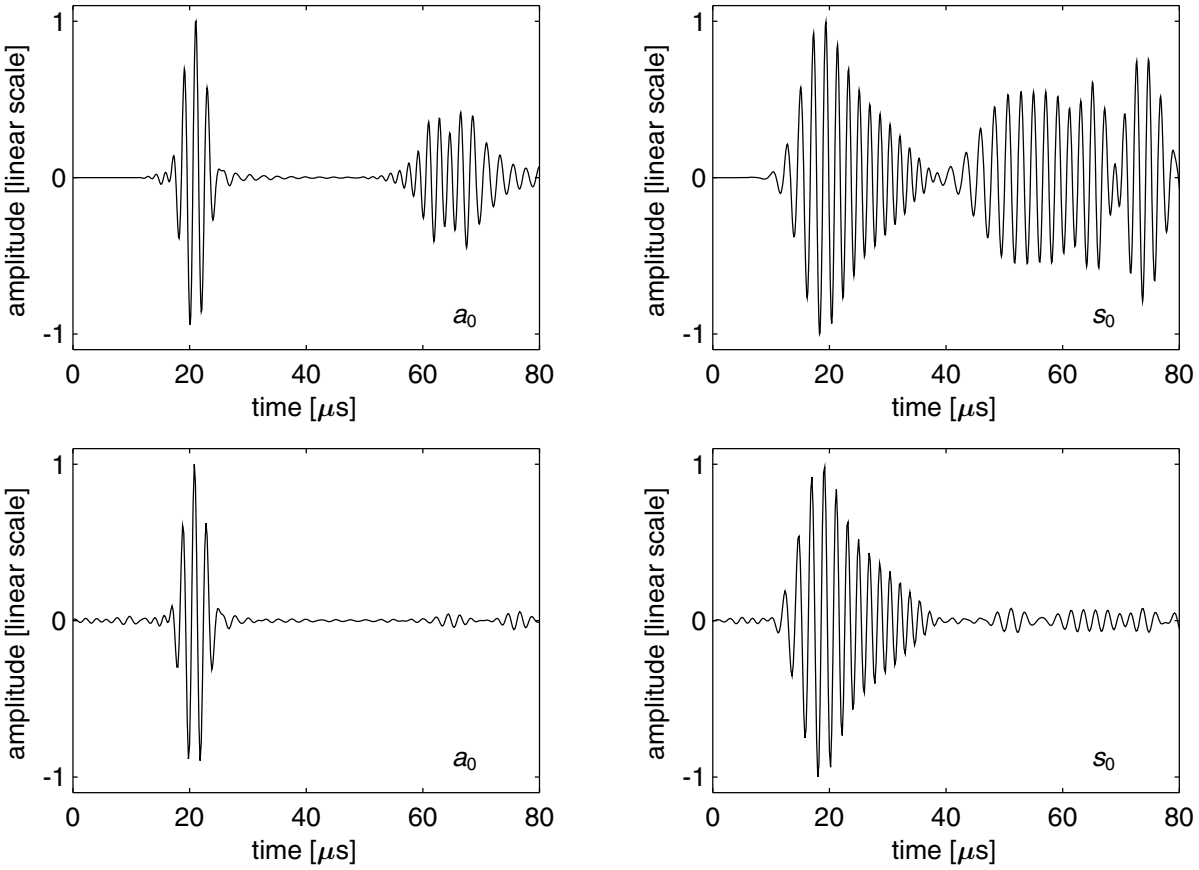

Fig. 13. Temporal waveform corresponding to the normal displacement at position $x = 50$ mm. Temporal method (upper plots) and frequency method (lower plots)

6. Conclusion

This paper reports on methods for determination of Lamb wave dispersion curves. Both algorithm working in the frequency domain and algorithm working in the more conventional temporal domain is possible to use for the estimate of dispersion curves also for other geometries than only thick plate.

Since a small number of frequencies are sufficient to achieve a correct representation of a wide variety of temporal excitations, the frequency method considerably speeds up the computation by avoiding the temporal FT and by decreasing the number of calculation steps.

Number of degrees of freedom for time method is 16 354 and for frequency method is 19 074. Number of elements for time method is 1 920 and for frequency method is 2 240. Higher values for frequency method are caused by presence of absorbing part. Despite of this fact the computation by frequency method is approximately 17 times faster then the computation by temporal method. The computations have also less requirements on the storage space of computer. Working in the frequency domain leads to FE calculations shorter than 90 seconds on a 2.67 GHz, 8-processor (Xeon Pentium), HP Workstation with 32 GB RAM.

The next advantage of this method is that the viscoelastic behavior could be taken into account by considering complex moduli as input data to the constitutive relations, since these are expressed in the frequency domain.

The frequency method can be also used for calculation of the temporal waveform of displacements. Temporal waveforms can be then reconstructed by applying the inverse FT to the set of harmonic displacements predicted for the given frequencies by FEM software. Fig. 13

shows the signal corresponding to the normal displacement predicted at position $x = 50\,\mathrm{mm}$. The case when the input at $x = 0$ was designed to excite only a_0 is depicted in the left plots and the case when the input at $x = 0$ was designed to excite only s_0 is shown in the right plots. Upper plots are results of transient analysis in FEM and lower ones are results of frequency analysis in FEM and following by the inverse FT. Note that the reflected waves are soften due to the absorbing part of the plate.

Acknowledgements

The work has been supported by the Institute Research Plan AV0Z20760514 and by the grants GA CR No 101/09/1630. Authors thank Michal Landa from the Institute of Thermomechanics AS CR for the experimental data.

References

[1] Alleyne, D. N., Cawley, P., A two-dimensional Fourier transform method for the measurement of propagateing multimode signals, Journal of the Acoustical Society of America 89 (3) (1991) 1 159–1 168.

[2] Alleyne, D. N., The nondestructive testing of plates using ultrasonic Lamb waves, Ph.D. thesis, Imperial College of Science, Technology and Medicine, London, 1991.

[3] Castaings, M., Bacon, C., Hosten, B., Finite element predictions for the dynamic response of two thermo–viscoelastic material structures, Journal of the Acoustical Society of America 115 (3) (2004) 1 125–1 133.

[4] Cheung, Y. K., Tham, L. G., Finite strip method, CRC Press, 1997.

[5] COMSOL, Inc., http://www.comsol.com.

[6] Delsanto, P. P., Chaskelis, H. H., Whitcombe, T., Mignogna, R. B., Connection machine simulation of boundary effects in ultrasonic NDE, In Nondestructive Characterization of Materials IV, Plenum Press, 1991.

[7] Graff, K. F., Wave motion in elastic solids, Dover, New York, 1991.

[8] Hesthaven, J., Gottlieb, S., Gottlieb, D., Spectral methods for time-dependent problems, Cambridge UK, 2007.

[9] Knopoff, L., A matrix method for elastic wave problems, Bulletin of the Seismological Society of America 54 (1) (1964) 431–438.

[10] Krautkrämer, J., Krautkrämer, H., Ultrasonic testing of materials, American Society for Testing and Materials, Springer, New York, 1990.

[11] Miklowitz, J., The theory of elastic waves and waveguides, North-Holland, Amsterdam, 1978.

[12] The MathWorks, Inc., http://www.mathworks.com.

[13] Yim, H., Sohn, Y., Numerical simulation and visualization of elastic waves using mass-spring lattice model, Transactions on Ultrasonics, Ferroelectrics and Frequency Control 47 (3) (2000) 549–558.